The Journal of Experimental Biology 206, 399-409

doi:10.1242/jeb.00074



# Expression and localization of carbonic anhydrase and ATPases in the symbiotic tubeworm *Riftia pachyptila*

Marie-Cécile De Cian*, Ann C. Andersen, Xavier Bailly and François H. Lallier

*Equipe Ecophysiologie, CNRS-UPMC UMR 7127 CEOBM, Station Biologique, BP 74, F-29682 Roscoff Cedex, France*

*Author for correspondence (e-mail: decian@sb-roscoff.fr)

*Accepted 14 October 2002*

**Summary**

**The symbiotic tubeworm *Riftia pachyptila* needs to fuel its chemoautotrophic symbiotic bacteria with inorganic carbon. $CO_2$ is transported from the surrounding water to the bacteriocytes located in the trophosome, through the branchial plume and the body fluids. Previous studies have demonstrated the implication of carbonic anhydrase (CA) and proton pumps (ATPases) at various steps of $CO_2$ transport. The present study describes the expression pattern of cytosolic CA using an RNA probe and its histochemical and immunocytochemical localization in the trophosome and branchial plume of *Riftia*. Immunolocalization of V-$H^+$ATPase and $Na^+K^+$-ATPase were also performed and related to CA localization. In the branchial plume, CA is expressed and localized in the most apical region of the branchial epithelium, close to the surrounding water. V-$H^+$ATPase is mostly colocalized with CA and both enzymes probably allow $CO_2$ entry against the concentration gradient while regulating intracellular pH. $Na^+K^+$-ATPase is mostly restricted to the basal part of epithelial cells and probably participates in $CO_2$ transport to the body fluids. In the trophosome lobules, cytosolic CA is expressed and found in bacteriocytes and peritoneal cells. Hypotheses on the role of CA in bicarbonate and $CO_2$ interconversion to fuel the symbiotic bacteria are discussed.**

Key words: Vestimentifera, carbonic anhydrase, V-$H^+$ATPase, $Na^+K^+$-ATPase, immunolocalization, *in situ* hybridization.

## Introduction

Carbonic anhydrases (CAs) are important enzymes (E.C.4.2.1.1) commonly produced by a variety of tissues, where they participate in a broad range of physiological processes such as acid–base homeostasis, carbon dioxide and ion transport and respiration (Henry, 1996). They catalyze the reversible conversion of bicarbonate and hydrogen ions into carbon dioxide ($CO_2$) and water. CAs are synthesized in a large number of tissues in animals, from mammals (Maren, 1967) to amphibian (Tufts et al., 1999) and fish (Henry et al., 1997). CAs have also been described in most invertebrate phyla studied, from cnidarians (Lucas and Knapp, 1996; Weis, 1991) to crustaceans (Henry and Cameron, 1982), to name a few.

The work described herein focuses on CA and proteins involved in ion exchange processes in the giant hydrothermal vent tubeworm *Riftia pachyptila* Jones. Adults lack both mouth and gut (Jones, 1981) but, however, exhibit the highest growth rates among marine animals (Lutz et al., 1994). They actually derive all their nutritional needs from the large population of sulfur-oxidizing chemolithoautotrophic bacterial symbionts that live in cells within a specialized organ located in their trunk, the trophosome (Cavanaugh et al., 1981; Felbeck, 1981). The trophosome is a soft tissue, composed of highly vascularized lobules, and surrounded by coelomic fluid (Jones, 1988). Because the bacterial symbionts are remote from the external milieu, the worm must take up sulfide, oxygen, nitrate and carbon dioxide from the environment and transport these inorganic molecules to the symbionts. All these substances are taken up from the surrounding water through the large and highly vascularized plume (Fig. 1) (Jones, 1988). They are transported by circulating fluids to provide energy, carbon and nitrogen source to the bacterial metabolic cycles, and ultimately transferred to the worm as organic molecules. As far as carbon dioxide is concerned, a number of studies have shown that molecular $CO_2$ enters by diffusion (Goffredi et al., 1997), and accumulates at very high concentrations in the body fluids (up to 30 mmol $l^{-1}$) (Childress et al., 1993). Transport of $CO_2$ in body fluids is mainly as bicarbonate, a limited amount being bound to the extracellular hemoglobins (Toulmond et al., 1994). However, the bacteria *per se* can only utilize molecular $CO_2$ (Scott et al., 1999). In addition, extracellular pH in the body fluids of *Riftia* remains very stable at approximately 7.3, despite these high amounts of carbon dioxide (Goffredi et al., 1997). As suggested by all these authors, carbon dioxide conversion is needed at various steps of the transport processes and probably involves high levels of carbonic anhydrase activity.

Previous studies biochemically characterized a functional cytoplasmic CA in the plume and in the trophosome of *Riftia*

(Kochevar et al., 1993), and other studies have also quantified V-$H^+$ATPase and $Na^+K^+$-ATPase activities in several tissues of *R. pachyptila* (Goffredi and Childress, 2001; Goffredi et al., 1999a). According to Goffredi and Childress (2001), *Riftia* regulates acid–base balance mainly *via* high concentrations of ATPases, 7–55% higher than other deep-sea (*Tevnia jerichonana*, *Calyptogena magnifica* and *Coryphaeniodes acrolepis*) and shallow-living (*Arenicola marina*, *Urechis caupo*, *Chaetopterus veriodepatus* and *Themiste pyroides*) animals. The authors also emphasized the importance of the $Na^+/H^+$ exchanger and $Na^+K^+$-ATPase in proton elimination and extracellular pH regulation in the face of the numerous processes acting to acidify the internal environment in the tubeworm. Moreover, a recent physiological investigation on isolated bacteriocyte suspensions from the trophosome tissue of *Riftia* revealed the complex interaction of carbonic anhydrase with two important ion-transporting enzymes, the vacuolar-type V-$H^+$ATPase and the $Na^+K^+$-ATPase. Both enzymes seem to be involved in the transepithelial transport processes for electrolytes and carbon dioxide (De Cian et al., 2002). These results suggest that in the trophosome, the proton motive force of the $H^+$ATPase drives transport processes involved in $CO_2/HCO_3^-$ (and possibly $HS^-$ transport) across the cell membrane by generating local acidification of the outer layer of the membrane. In this symbiotic tissue the relative importance of $H^+$ATPase minimizes the role of $Na^+K^+$-ATPase in ion equilibrium. However, $Na^+K^+$-ATPase is likely to play an important role in the plume.

These physiological results prompted us to investigate the respective localization of the various proteins involved, in order to better understand carbon dioxide transport, conversion and incorporation processes that are specific to this symbiosis. The present study describes the expression pattern of cytosolic CA using an RNA probe and its histochemical and immunocytochemical localization in the trophosome and other non-symbiotic tissues of *R. pachyptila*. Immunolocalization of the two ion transporter enzymes V-$H^+$ATPase and $Na^+K^+$-ATPase were also investigated and related to CA localization.

## Materials and methods

### *Animals*

Juvenile specimens of *Riftia pachyptila* Jones were collected at 9°N (9°50′N, 104°18′W) and 13°N (12°48′N, 103°57′W) hydrothermal vent sites (2600 m depth) along the East Pacific Rise during the HOPE 99 cruise. Animals were collected with the telemanipulated arm of the submersible *Nautile* and brought to the surface in a temperature-insulated container. Upon their arrival onboard, small individuals (<5 cm) were removed from the surface of a few adult tubes and immediately transferred to chilled seawater (5°C) in a refrigerated container. Selected specimens were removed from their tube and checked for tactile responsiveness prior to fixation procedure.

### *Protein extraction*

Plume, vestimentum, body wall and trophosome tissues were dissected onboard immediately after recovery of the animals, washed several times with *Riftia* saline (Fisher et al., 1988) and frozen separately into liquid nitrogen until used. Membrane and crude homogenates were prepared from 1 g of frozen tissue of each body part. The tissues were homogenized on ice using a Tissuemizer (Ultra-Turrax, Janke-Kuntel, Ika Labortechnik, Staufen) by three 30 s bursts in 4 ml extraction buffer. The extraction buffer contained 50 mmol $l^{-1}$ Tris-HCl, pH 7.5, 200 mmol $l^{-1}$ sucrose, 150 mmol $l^{-1}$ KCl containing protease inhibitors including 2 mmol $l^{-1}$ EDTA, 1 mmol $l^{-1}$ Pefablock (Boehringer Mannheim), 5 μg $ml^{-1}$ chymostatin, 10 μg $ml^{-1}$ leupeptin and 10 μg $ml^{-1}$ aprotinin. Samples were kept on ice during the whole procedure and centrifuged at 10 000 ***g*** for 20 min at 4°C. The supernatant (S1) was transferred in a new tube and stored at 4°C. The pellet was washed twice and then solubilized for 1 h in 2 ml of membrane buffer containing 1% Triton X-100 (3 vol.), Tris buffer used above (7 vol.) and 0.2% saponin (1 vol.) (Brion et al., 1997). Proteins were solubilized by breaking up the membrane pellet with a pipette tip, vortexing and sonicating. S1 and the solubilized pellet (P1) were then ultracentrifuged at 100 000 ***g*** for 1.5 h at 4°C resulting in supernatants S2 (from S1, soluble proteins) and S3 (from P1, membrane-associated proteins). The pellet P3 was solubilized one more time in 500 μl of the Triton X-100 buffer in the same conditions as above and ultracentrifuged at 100 000 ***g*** for 1.5 h at 4°C, but the resulting supernatant did not contain significant amount of proteins. All samples were stored in homogenization buffer with 5× Laemmli sample buffer at –40°C (Laemmli, 1970).

### *Western blots*

Protein concentrations were determined by the method of Bradford (1976). 7 μg of protein from each fraction were loaded on reducing SDS-PAGE gels for silver nitrate staining and 30 μg were loaded in triplicates for western blotting (Brion et al., 1997). Proteins were transferred to a nitrocellulose (Bio-Rad) membrane using a wet (Tris–glycine–20% methanol) transfer unit for 2 h at 4°C and 80 V. All blocking and antiserum incubations were done in TBST (20 mmol $l^{-1}$ Tris-HCl, pH 7.5, 0.5 mol $l^{-1}$ NaCl, 0.05% Tween 20). After blocking for 2 h in 5% skimmed milk in TBST at room temperature, the membrane was split up into three identical parts. Each one was incubated overnight at 4°C with a different primary antibody: (i) rabbit anti-chick 30 kDa CA-II (a generous gift from Dr P. Linser, Whitney Laboratory, University of Florida, St Augustine, USA) diluted 1:1000, (ii) mouse monoclonal antibody raised against the 60 kDa β-subunit of yeast V-$H^+$ATPase (Molecular Probes) diluted 1:500, and (iii) ‘α5’ ascites diluted 1:1000. The primary antibody ‘α5’, developed by Douglas M. Fambrough, was obtained from the Developmental Studies Hybridoma Bank developed under the auspices of the National Institute of Child Health and Development and maintained by The University of Iowa, Department of Biological Sciences, Iowa City, IA 52242, USA. This antibody was raised against chicken $Na^+K^+$-ATPase α-subunit, a 1020-amino-acid membrane

protein, with a large spectrum of cross-reactions recorded from mammals to insect and frog (Lebovitz et al., 1989). As positive standard for CA we used bovine CA, present in the molecular mass marker mix (LMW electrophoresis calibration kit, Amersham Pharmacia Biotech., France). Pre-immune rabbit serum (Sigma) and omission of the primary antibody were used as negative controls. The membrane was then rinsed 3 times in TBST and incubated for 2 h at room temperature with a 1:3000 dilution of pig anti-rabbit horseradish peroxidase-conjugated IgG antibody (DAKO A/S, Denmark) or sheep anti-mouse HRP-conjugated IgG antibody (Amersham Pharmacia Biotech.). The antigen–antibody complex was revealed by the chemiluminescence system (ECL, Amersham Pharmacia Biotech., France) according to the manufacturer's instructions, and by exposing autoradiographic film X-OMAT AR (Eastman Kodak Co. NY, USA) to the nitrocellulose membrane.

### *Preparation of the probes for* in situ *hybridization*

The plasmid carrying *Riftia* CA cDNA (EMBL accession number AJ439711; 356-378 bp fragment) was linearised appropriately for either T7 or T3 polymerase-directed RNA synthesis. Synthesized RNA was labeled by incorporating digoxigenin (DIG)-conjugated UTP, as recommended by the manufacturer (Boehringer-Mannheim). The following solutions were added to 1 μg of linearized template: 2 μl of a 10 mmol $l^{-1}$ nucleotide mix (including 3.5 mmol $l^{-1}$ labeled UTP and 6.5 mmol $l^{-1}$ unlabeled UTP), 2 μl of 10× transcription reaction buffer, 1 μl of RNase Inhibitor, 2 μl of the specific polymerase and DEPC (diethyl pyrocarbonate) water to 20 μl final volume. After 2 h at 37°C, 2 μl of DNase I RNase-free was added to digest the cDNA template and 2 μl of 0.5 mol $l^{-1}$ EDTA was added to end the transcription reaction. CA sense and antisense mRNAs were purified onto Quickspin columns (Boehringer-Mannheim) and stored in the elution buffer (300–500 ng samples in 5 μl) at –80°C.

### In situ *hybridization*

Small entire juveniles or tissue pieces 5 mm thick were fixed in 0.1 mol $l^{-1}$ phosphate-buffered 4% paraformaldehyde (pH 7.4) for 4 h at 4°C. After rinsing in 100 mmol $l^{-1}$ phosphate buffer (PB) three times, the specimens were dehydrated in an ethanol series and embedded in paraffin wax. Sections (5–7 μm) were collected on Biobond (BBInternational, Cardiff, UK) coated glass slides and air-dried overnight at 40°C. The sections were dewaxed in toluene, rehydrated in an ethanol series and washed in PBS. They were then post-fixed in 4% paraformaldehyde in PBS for 15 min at room temperature, deproteinized for 10 min with 0.2 mol $l^{-1}$ HCl, treated for 10 min in 2× SSC at 70°C, and rinsed in PBS, 0.1 mol $l^{-1}$ triethanolamine acid, pH 8, containing 0.5% acetic anhydride under agitation at room temperature. Slides were then incubated with 50 μg $ml^{-1}$ proteinase K for 15 min at 37°C in a wet chamber, rinsed in PBS, and eventually dehydrated in an ethanol series, air-dried, stored at –80°C and used within 2 weeks after pre-treatment. All these steps were carried under RNase-free conditions with RNase-free products, all provided by Sigma-Aldrich.

Hybridization specificity and optimal conditions of the RNA probes were tested on dot blots (data not shown) using total RNA of *R. pachyptila* tissues as a matrix. Sections were pre-hybridized at 45°C for 1 h in hybridization buffer (50% deionized formamide, 0.9 mol $l^{-1}$ NaCl, 20 mmol $l^{-1}$ Tris-HCl, pH 7.5, 0.01% SDS, 2% blocking reagent (Boehringer-Mannheim), and hybridized with DIG-labeled CA riboprobes (100 ng/slide) overnight at 45°C in a wet chamber with a coverslip. Experimental tissue sections were hybridized with the anti-sense CA riboprobe and control sections with the sense riboprobe. After stringent washing (20 mmol $l^{-1}$ Tris-HCl, pH 7.5, 28 mmol $l^{-1}$ NaCl, 0.01% SDS, 5 mmol $l^{-1}$ EDTA) at 47°C for 20 min, immunological detection was performed with DIG Nucleic Acid Detection Kit [sheep anti-DIG-alkaline phosphatase (Fab fragments), and NBT/BCIP as a substrate; Boehringer-Mannheim] according to the manufacturer's instructions.

### *Immunocytochemistry*

Tissue pieces or juveniles (2–10 cm long) were fixed in cold methanol at –20°C and then cryo-embedded in tissue-teck or embedded in paraffin wax as described above. Cryosections (7 μm) were cut on a Microm cryotome at –25°C, collected on glass slides coated with 1% gelatin, air-dried at room temperature and then stored at –40°C. When used, the sections were first postfixed in methanol containing 0.3% $H_2O_2$ to inhibit endogenous peroxidase activity, and rinsed in PBS (10 mmol $l^{-1}$ sodium phosphate buffer, pH 7.4, 150 mmol $l^{-1}$ NaCl). Sections were then incubated in blocking solution [10% normal goat serum (NGS), 1% BSA, 0.3% Tween 20 in PBS] for 1 h prior to application of the primary antibody. The primary antibodies, i.e. polyclonal anti-CAII, monoclonal anti V-$H^+$ATPase or monoclonal 'α5', were diluted 1:50 in PBS containing 1% NGS, 1% BSA, 0.3% Tween 20 (Carrier Solution, CS). The slides were incubated for 2 h in a moist chamber at 37°C. The sections were then rinsed in CS, and incubated with a 1:100 in CS HRP-labeled anti-mouse for monoclonal antibodies (DAKO), or fluorescein-conjugated goat anti-rabbit IgG secondary antibody for CA antibody (Sigma), for 1 h at room temperature. After washing with CS, monoclonal antibody binding was visualized by applying a solution of 4-chloro-1-naphthol (ImmunoPure, Pierce Biotech., Rockford, IL, USA) until emergence of the characteristic purple-blue color. Sections treated with CA antibody were mounted in antifading reagent AF3 (Citifluor Ltd, London).

### *Histochemical detection of carbonic anhydrase by fluorescence*

The CA enzyme was detected with 1-dimethylamino-naphthalene-5-sulfonamide (DNSA), a fluorescent inhibitor with a great affinity for the catalytic center of CA (Chen and Kernohan, 1967; Dermietzel et al., 1985). The emission wavelength of DNSA shifts from 580 to 468 nm when binding to CA. The trophosome, plume and vestimentum tissue pieces

were rinsed in Riftia saline (Fisher et al., 1988) and immediately frozen in liquid nitrogen. Cryostat sections (10 µm in thickness) were prepared at –27°C, transferred to poly-L-lysine coated slides (Sigma) and fixed with a drop of cold methanol (–20°C) before thawing (Just and Walz, 1994). Immediately after methanol evaporation, sections were stained with 0.1 mmol $l^{-1}$ DNSA (Sigma) in phosphate buffer in a wet chamber at room temperature for 30 min, then mounted in PB (Dermietzel et al., 1985). In control experiments, non-fluorescent CA inhibitors acetazolamide (AZ) or ethoxyzolamide (EZ), both provided by Sigma-Aldrich, were added to the incubation medium at a concentration of 1 mmol $l^{-1}$.

### *Microscopy and image acquisition*

*In situ* hybridizations were observed on a Leitz Laborlux D light microscope. Slides used for immunocytolocalization were observed with an Olympus BH-2 epifluorescence microscope (Olympus Optical Co. Tokyo, Japan) equipped with a mercury light source and a ×40 UVFL objective (excitation/emission filters: 490/515 for fluoroisothiocyanate). Micrographs were taken with Kodak films P160 (tungsten light) or P1600 (fluorescence).

Slides used for histolocalization of CA were observed with a Confocal Laser Scanning Biological Microscope (CLSM, Fluoview, Olympus Optical Co. Ltd, Tokyo, Japan). Optical sections (0.7 µm) were taken through bacteriocytes with the CLSM equipped with a pulsed laser (Mira 900, Coherent, Santa Clara, CA, USA) to obtain an equivalent biphoton excitation at 380 nm and at 470 nm. The 470 nm barrier filter (bandwidth 10 nm) allows the detection of the blue fluorescence of the CA-bound DNSA (maximum emission at 468 nm), but shuts down the yellow-green fluorescence of unbound DNSA (maximum emission at 580 nm; Chen and Kernohan, 1967).

Micrographs were processed with Adobe Photoshop 5.5 (Adobe Systems Inc., San José, USA) and NIH Image (http://rsb.info.nih.gov/nih-image) where appropriate.

## Results

Fig. 1 shows the different body compartments of *Riftia*, and their pattern of total RNA synthesis, detected by Gallocyanin staining. Tissues showing the darker coloration are the trophosome, together with the internal branchial filaments where these are fused into lamellae (Andersen et al., 2002), and the body wall in the vestimentum and trunk, where dark spots visible at the edge of the vestimentum wings and, more discretely, along the body wall, might correspond to the pyriform glands, the sites of chitin production (Shillito et al., 1995). These four tissues, branchial plume, vestimentum, trunk body wall and trophosome, were thus the obvious targets to check the validity of our antibodies and the presence of the proteins of interest. This step was necessary because of the lack of biochemical and molecular tools specific to invertebrates, which led us to use different antibodies, raised in commonly used models for immunological studies.

### *Identification of CA and ATPases*

Western blot analyses were performed on total soluble and

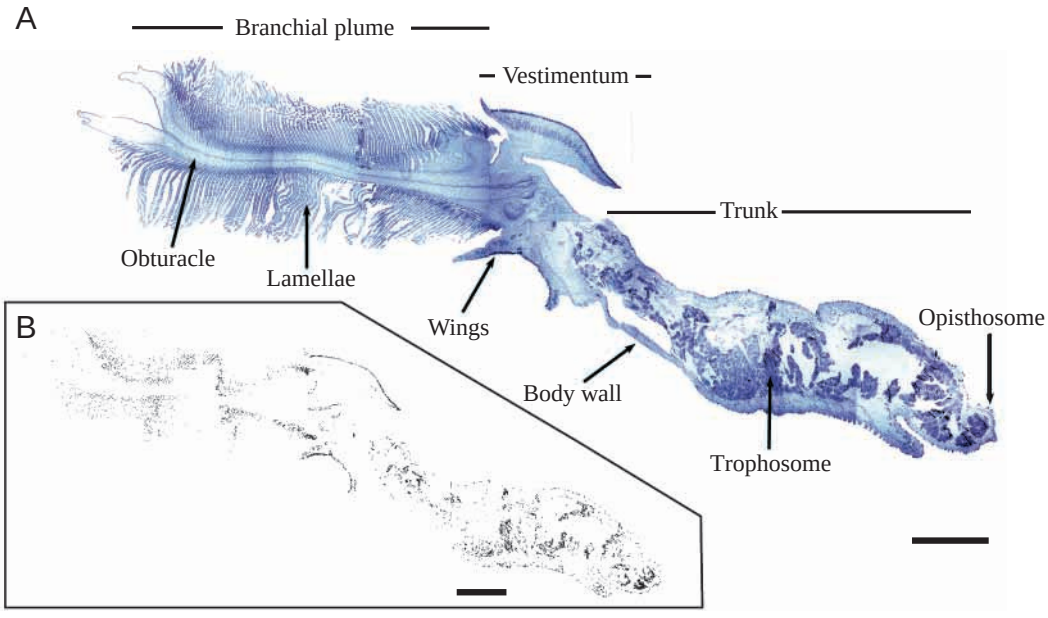


Fig. 1. (A) Sagittal section showing the body parts of the whole vestimentiferan tubeworm *Riftia pachyptila* and the labeling of total RNA by Gallocyanin. The four main body compartments of the worm are indicated, with their respective RNA synthesis activity. (B) Corresponding densitometry analysis of the section processed with NIH Image, with a binary transform at 50% threshold. Maximal transcription activity was detected in the trophosome lobules, at the basis of the joined branchial lamellae and in the epithelium of the wings. The obturaculum, vestimentum and body wall showed basal expression levels. Scale bar, 2 mm.

membrane-associated protein extracts from the four main tissues of *Riftia* for CA (Fig. 2) and from branchial plume and trophosome for the ion transporters (Fig. 3). Fig. 2A shows the specific protein patterns of each tissue as revealed by silver nitrate staining. The vestimentum and the body wall exhibited very similar patterns for both soluble and membrane-associated protein fractions, and differed from the plume protein profile by several major bands. Meanwhile, the proteins constituting the symbiotic tissue appeared different from the other three tissues. Polyclonal rabbit antibody raised against chick 30 kDa CA cross-reacted with a 27 kDa cytosolic protein in the plume and a 28 kDa cytosolic protein in the trophosome (Fig. 2B). This antibody did not cross-react with any other protein in the four tissues tested. The α5 monoclonal antibody raised against a chicken 1020-amino-acid $Na^+K^+$-ATPase cross-reacted with membrane-associated proteins only, labeling two bands in the trophosome and three bands in the plume, all of them with a molecular mass of 115 kDa (Fig. 3A). The monoclonal antibody raised against yeast 60 kDa β-subunit of V-$H^+$ATPase cross-reacted with proteins from the membrane fraction (S3), producing two distinct bands of 59 and 57 kDa in the plume and one band of 57 kDa in the trophosome (Fig. 3B). A lighter band appears in the cytosolic fraction (S2) in both tissues, at 59 kDa in the plume and at 57 kDa in the trophosome.

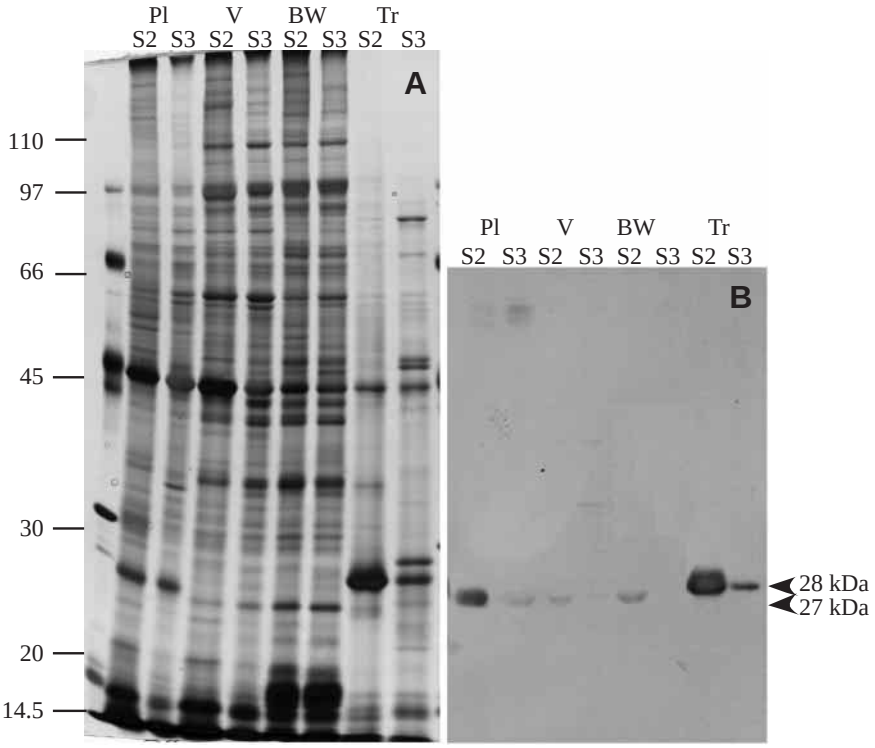


Fig. 2. (A) SDS-polyacrylamide gel of total protein extracts of *Riftia pachyptila* tissues (load approx. 7 µg) stained with silver nitrate, and (B) corresponding immunoblot probed with rabbit anti-chick CA II. CA cross-reacted with a protein of a 27 kDa in the plume and one of 28 kDa in the trophosome. The vestimentum and the trunk body wall were weakly immunoreactive to CA antibody. No cross-reaction was observed with pre-immune serum (data not shown). The positions of marker proteins (kDa) are shown. BW, body wall; Pl, plume; S2, soluble protein fraction; S3, membrane-associated protein fraction; Tr, Trophosome; V, vestimentum.

*CA localization*

To identify the expression of CA genes in the tissues of *R. pachyptila*, degenerate oligonucleotide primers (Table 1) were designed on the basis of conserved regions in published cDNA sequences coding for cytosolic, membrane-associated, mitochondrial and secreted CA in a wide range of species. A cDNA sequence of 225 nucleotides was amplified, cloned and identified *via* BLAST search of GenBank as a cytosolic-like CA fragment. This cloned fragment was checked for specificity by northern blot (not shown), and then used for *in situ* hybridization experiments. Hybridization experiments with the CA antisense probe and immunolocalization on transverse sections showed an intense label in the trophosome (Fig. 4) and the branchial filaments (Fig. 5).

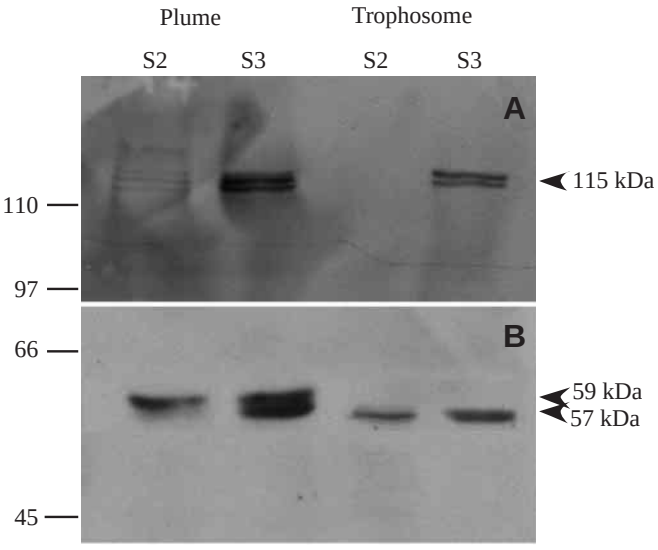


Fig. 3. (A) Western blot analysis of $Na^+K^+$-ATPase. Proteins of molecular mass approx. 115 kDa were probed with anti-chicken $Na^+K^+$-ATPase antibody in the plume and in the trophosome membrane fractions (S3) but not in the soluble fractions (S2). (B) Western blot analysis of V-$H^+$ATPase. Two bands of approximately 59 and 57 kDa were visualized with anti-yeast V-$H^+$ATPase antibody for the plume fraction, but only one band of 57 kDa in the trophosome. The positions of marker proteins (kDa) are shown.

Table 1. *Oligonucleotide primers employed to amplify carbonic anhydrase fragment used for* in situ *hybridization with riboprobe*

| Primer set | Nucleotide sequence (5′→3′) | Position in cDNA of *A. elegantissima* |
|---|---|---|
| Degenerate sense primer CA4A | GAG CAR TTY CAY TTY CAY TGG | 282–303 |
| Degenerate antisense primer CA8 | CGG ART ANG TCC ART ART C | 582–601 |

*Anthopleura elegantissima* carbonic anhydrase cDNA GenBank Accession number: AF140537.
N, A/C/G/T; R, A/G; Y, C/T.

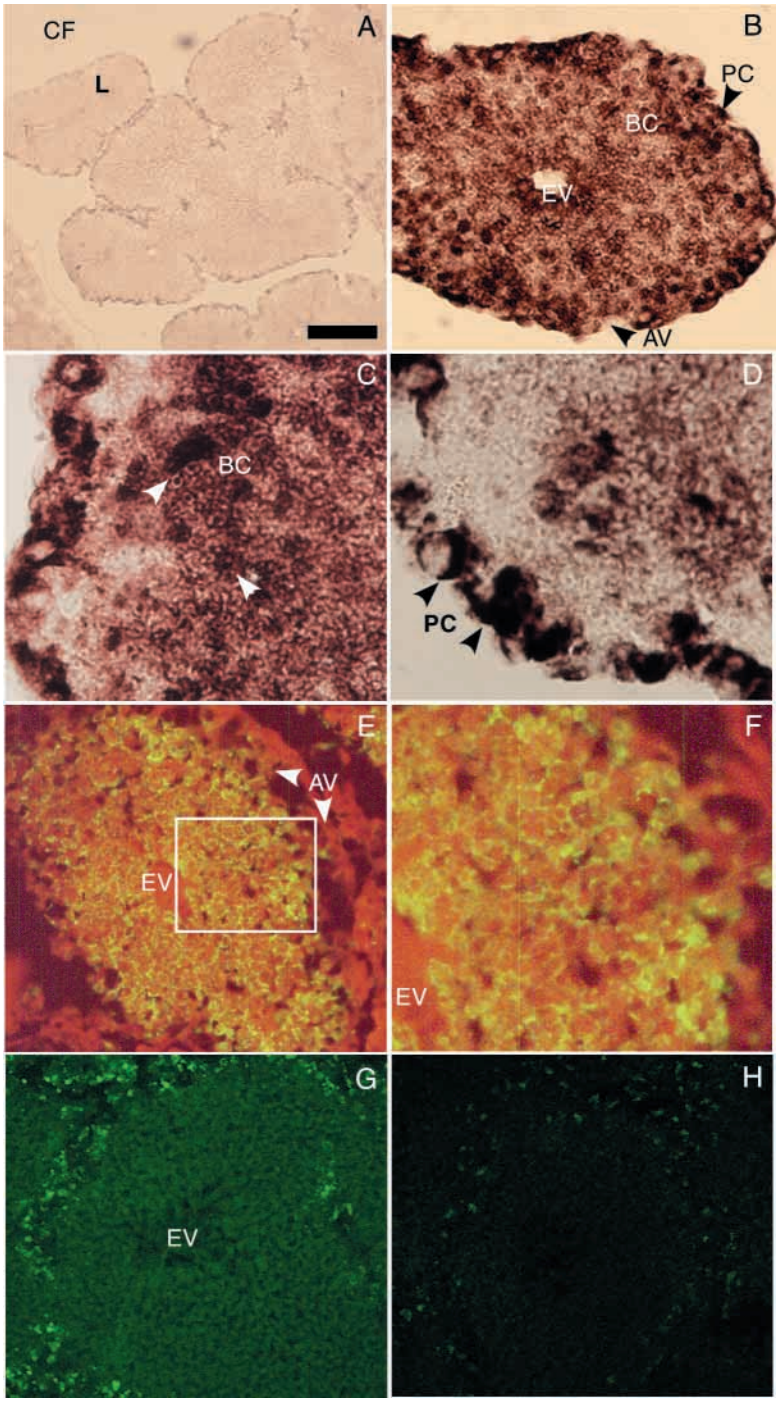


The trophosome consists of numerous lobules, each of these being a functional unit (Fig. 4A). Each lobule is provided with an axial efferent blood vessel, several afferent vessels situated at the periphery of the lobule, and many capillaries joining them. Four cell types make up the trophosome lobules: non-bacteriocyte cells, either (i) unspecialized cells or (ii) muscle cells in the external layer immediately adjacent to the axial vessel; (iii) bacteriocytes filling the whole central part of the lobule, and (iv) a layer of peritoneal cells in the outermost region. The bacteriocytes are the specialized cells containing the chemosynthetic bacteria within vacuoles. No label was found in the controls incubated with sense riboprobe (Fig. 4A). Cytosolic CA mRNA was consistently found in all lobules, except for blood vessels (Fig. 4B). Close-ups show that both the bacteriocytes and the peritoneal cells are labelled (Fig. 4C,D). The intensity of the label was often weaker in the bacteriocytes compared to the peritoneal cells (Fig. 4D). Protein immunoreactivity was also apparent in all trophosome lobules from the inner to the outer part (Fig. 4E). The central efferent vessel and the peripheral afferent vessels were all free of staining (Fig. 4E). The intensity of the green label was maximum around the intracellular bacteria, which appeared in red (Fig. 4F). Using DNSA, a fluorescent, specific inhibitor of CA, the cytoplasm

Fig. 4. Localization of carbonic anhydrase in trophosome lobules of *Riftia pachyptila.* (A–D) *In situ* hybridization of carbonic anhydrase mRNA with DIG-labeled riboprobe. (A) Negative control, showing the organization of the trophosome with numerous lobules (L) bathing in coelomic fluid (CF). (B–D) Section of a lobule composed of a central efferent vessel (EV), peripheral afferent vessels (AV), bacteriocytes (BC) and peritoneal cells (PC) in the extreme periphery of the lobule. Arrowheads indicate positive hybridization with the riboprobe in the bacteriocytes (C) and in the peritoneal cells (D). (E) Corresponding protein immunolocalization using rabbit anti-chick CA II antiserum with (F) a detailed portion (boxed area in E) focusing on CA labeling in the bacteriocytes filling the lobule. (G,H) Histochemical localization of CA with DNSA (G) and corresponding result of competition with Ethoxyzolamide (H). Scale bar, 150 μm (A); 50 μm (B,E,G,H); 15 μm (C,D,F).

of the peritoneal cells showed a bright fluorescence, owing to the formation of the enzyme–substrate complex between CA and DNSA (Fig. 4G). When ethoxyzolamide, the non-fluorescent competitor of DNSA, was added to the incubation medium, a dose- and time-dependent disappearance of the fluorescence was observed, until the fluorescence was completely abolished (Fig. 4H).

The same study was performed on the non-symbiotic tissues of the worm: the trunk body wall, vestimentum and plume. CA mRNA hybridization experiments in the body wall and in the vestimentum only gave weak signals, thus we chose to focus our results on CA expression and immunolocalization in the branchial plume. It is a conspicuous organ, held rigid by the axial collagenous obturaculum, and composed of many rows of lamellae formed by contiguous filaments (Fig. 5A). The free distal tip of each filament bears, on its posterior side, two close rows of pinnules (Fig. 5B). Each filament contains an afferent and an efferent blood vessel bathing in coelomic fluid (Fig. 5D,E). Cytosolic CA mRNA hybridization was labeled in the epidermis of the branchial filaments, where the cells are in contact with the coelomic cavity, but also more apically (Fig. 5B,D). The connective tissue between joined lamellae was always free of staining (Fig. 5C), and only a weak signal could be detected directly around the afferent and efferent vessels (Fig. 5D). The enzyme itself appeared more specifically localized in the apical region of the epithelial cells, at the interface between environmental water and plume epidermis, as shown by immunolocalization with anti-chick CA-II (Fig. 5F). Indeed the expression of CA mRNA appeared to be enhanced in the pinnules of each filament (Fig. 5B), and the same intense staining was observed in immunolocalization experiments with anti-chick CA-II (data not shown). A similar pattern resulted from the fluorescence signal of CA-bound DNSA (Fig. 5G), which emphasized the apical side of the branchial epidermis. Controls performed with sense riboprobe (Fig. 5A), pre-immune serum (Fig. 5E) and competition with EZ (Fig. 5H) did not result in any aspecific background staining.

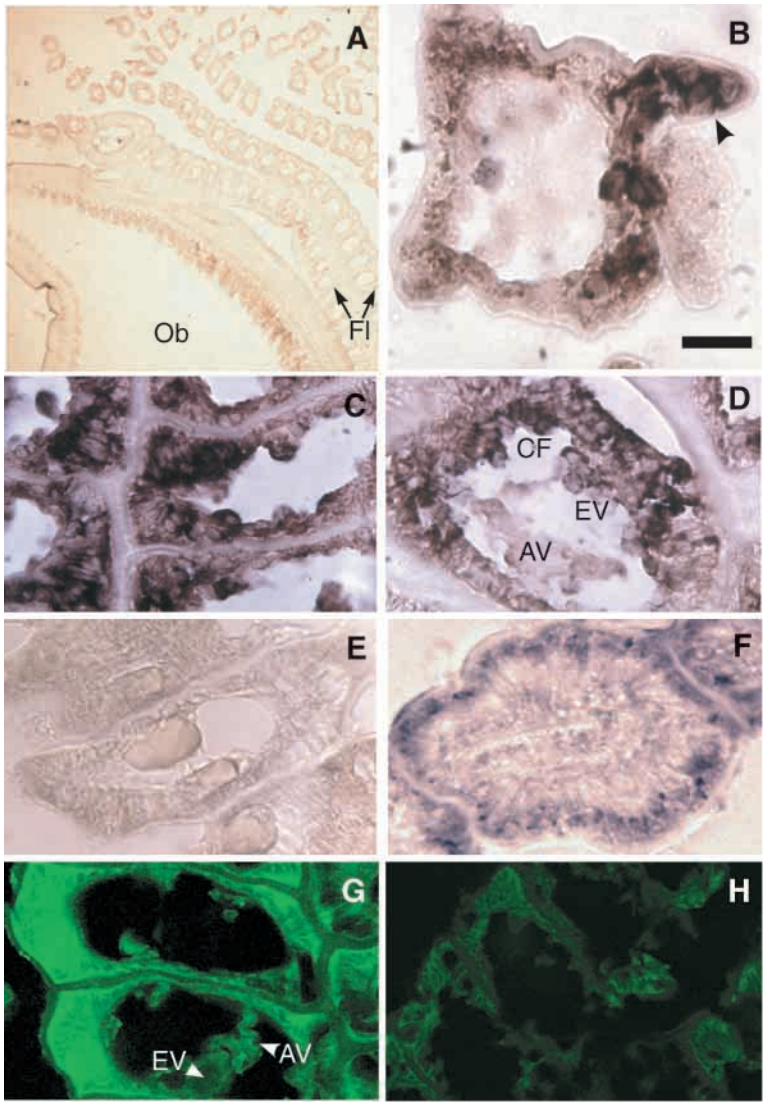


Fig. 5. Localization of carbonic anhydrase in branchial tissue of *Riftia pachyptila*. (A) Negative control with sense riboprobe on a transverse section of the plume showing its anatomical organisation. Lamellae are attached to the central obturaculum (Ob), and are composed of filaments (Fl) joined proximally but free distally. (B–D) *In situ* hybridization of CA mRNA with DIG-labeled riboprobe. (B) Transverse section of a single filament; the arrowhead indicates maximum staining intensity observed in a pinnule. (C,D) Epithelial cells are clearly stained by CA riboprobe, contrasting with the weak staining of extracellular matrix (C) and vascular vessels (D). (E) Negative control for CA immunolocalization using rabbit anti-chick CA II antiserum. (F) Corresponding protein immunolocalization restricted to the apical region of the epithelial cells. (G) Protein localization with DNSA, and (H) control section with DNSA on slides pre-incubated with the competitive CA inhibitor ethoxyzolamide. AV, afferent blood vessel; CF, coelomic fluid; EV, efferent blood vessel. Scale bar, 200 μm (A); 40 μm (E,G,H); 20 μm (B–D,F).

### *ATPase localization*

Immunolocalizations of V-$H^+$ATPase and $Na^+K^+$-ATPase were also investigated on trophosome lobules (Fig. 6) and branchial filaments (Fig. 7), to explore any possible colocalization of these two ion transporters with the cytosolic carbonic anhydrase visualized within the same tissues. Fig. 6A shows a cross-section of a trophosome lobule from the inner part, the efferent vessel, to the periphery, stained with DAPI. Dense blue-colored dots marked nuclei of the non-symbiotic cells, around the efferent vessel and in the outer part of the lobule, while bacteriocytes exhibited a more diffuse signal due to the staining of prokaryotic DNA. DAPI staining also distinguished pink-colored host cell membranes on the trophosome section, which were barely visible by light microscopy. Fig. 6B illustrates the corresponding immunolabeling with the

V-H$^+$ATPase antibody, showing bright label at the level of the bacteriocytes (Fig. 6B), but much less around peritoneal cells. Higher magnification of the bacteriocytes revealed that the label surrounds the bacteria (Fig. 6C). The use of Na$^+$K$^+$-ATPase antibody led to a signal that was mostly localized in bacteriocytes at the periphery of the lobules (Fig. 6D). The linear appearance of the label suggests its localization on membranes (Fig. 6E), although these were not clearly discernible.

In transverse sections of branchial filaments, the epithelial cells appeared to possess a V-H$^+$ATPase with localization restricted to the apical membrane and intracellular vesicles (Fig. 7A,B), and a densification of the vacuoles close to the apical area (Fig. 7B). Na$^+$K$^+$-ATPase immunostaining on plume filament cross sections was intense and restricted to the basolateral membrane of the cells surrounding the coelomic cavity containing the afferent and efferent vessels (Fig. 7C).

No staining was detected when pre-immune mouse or rabbit serums were used instead of primary antibody, either on trophosome lobules or on branchial filaments.

## Discussion

### *Antibody specificity*

CA, V-H$^+$ATPase and Na$^+$K$^+$-ATPase enzymes were detected in total protein extracts of the trophosome and branchial plume. The proteins that cross-reacted with the three antibodies had similar molecular mass to the corresponding proteins known in vertebrates, and they were the only immunoreactive proteins visualized on the immunoblots. Although not conclusive, these biochemical results showed that the antibodies used apparently detected the true respective proteins, and could be applied with some confidence for specific immunohistological localization on *Riftia pachyptila* tissue cross-sections. Such a strong immunoreactivity between anti-vertebrate antibodies and the target proteins in *Riftia* also

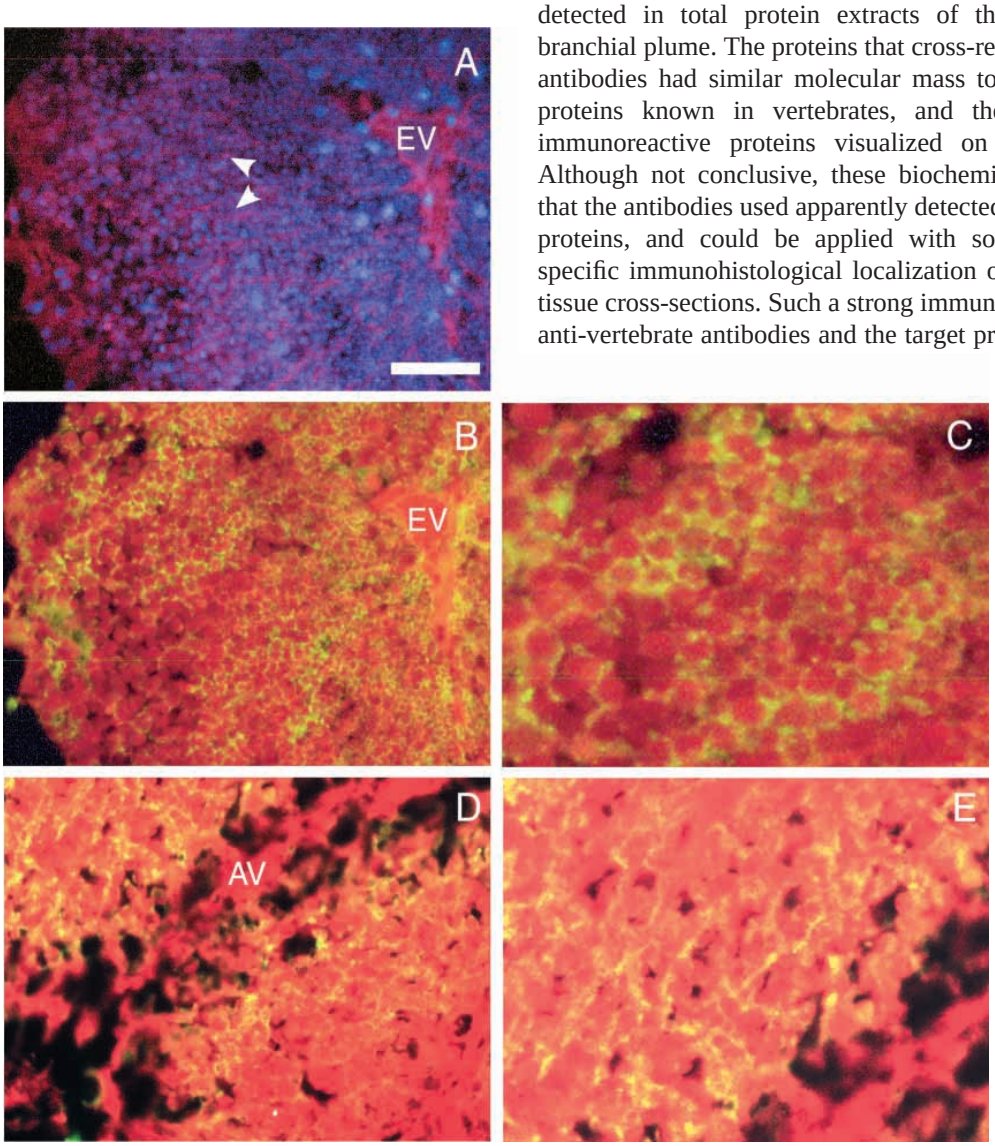


Fig. 6. Immunocytochemical analyses of V-H$^+$ATPase and Na$^+$K$^+$-ATPase in cryosections of trophosome of *Riftia pachyptila*. (A) Lobule section stained with DAPI. Bacteriocytes are characterized by a more diffuse staining than peritoneal cells and cells surrounding the efferent vessel (EV), due to the staining of bacterial DNA; white arrowheads indicate bacteriocyte cell membranes. (B) Corresponding section showing the immunolocalization of V-H$^+$ATPase in the lobule. Staining was abundant all around the bacterial vacuoles, membrane and vacuolar sublocalization being hardly distinguishable using light microscopy, even at higher magnification (C). (D,E) Immunolocalization of Na$^+$K$^+$-ATPase, where staining was restricted to the periphery of the lobule (D) and appeared to line host cell membranes (E). AV, afferent blood vessel; EV, efferent blood vessel. Scale bar, 20 μm (A,B,D); 6 μm (C,E).

suggests that these proteins are highly conserved members of these gene families. In addition, the nucleotide sequence of the cDNA fragment used for *in situ* hybridization revealed strong similarities with the α-CA gene family of vertebrates (data not shown).

The expression pattern of CA mRNA was analyzed in the branchial plume and trophosome of *Riftia pachyptila*, as well as the localization of the corresponding proteins. Evidence was also found for two ion pumps, type V-$H^+$ATPase and $Na^+K^+$-ATPase, which are functionally associated to CA (Goffredi and Childress, 2001; De Cian et al., 2002). How do the present results help our understanding of the overall transport processes of $CO_2$ in *Riftia*? Some of the major implications and hypotheses are discussed below.

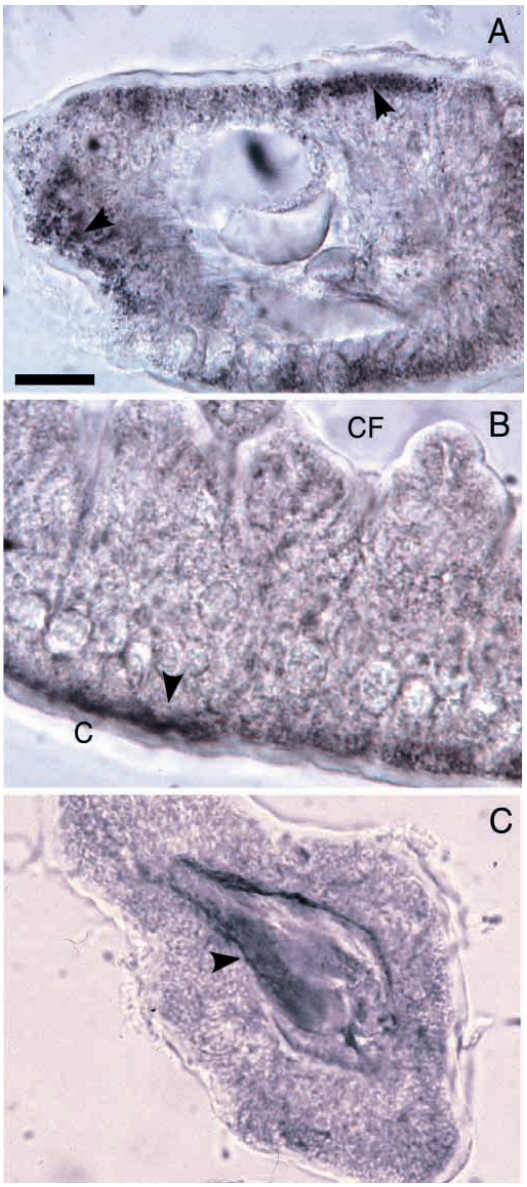


Fig. 7. Immunocytochemical analyses of V-$H^+$ATPase and $Na^+K^+$-ATPase in cryosections of the branchial filaments of *Riftia pachyptila*. (A) Transverse section of branchial filament stained for V-$H^+$ATPase. (B) Magnification of cell membrane area from A showing the apical localization of the V-$H^+$ATPase (arrowheads). (C) Localization of $Na^+K^+$-ATPase in transversal section of branchial filament showing its basal localization in the epidermis (arrowhead). CF, coelomic fluid; C, cuticle. Scale bar, 40 μm (A,C); 10 μm (B).

### *$CO_2$ transport across the branchial plume epithelium*

The branchial plume plays a key role in the physiology of *Riftia*, since it is the organ where almost all ion and metabolite exchanges take place, especially $CO_2$ incorporation and internal concentration processes. High activity levels of CA and ATPase have been reported in *R. pachyptila* plume tissue: 254 μmol $CO_2$ $min^{-1}$ $g^{-1}$ wet mass for CA (Goffredi et al., 1999b) and 646 μmol $P_i$ $h^{-1}$ $g^{-1}$ wet mass for total ATPase, 13% of which was attributed to $Na^+K^+$-ATPase, and 14% to V-$H^+$ATPase (Goffredi and Childress, 2001). Physiological studies have also demonstrated the importance of proton exclusion mechanisms as well as CA activity in maintaining an inward $CO_2$ flux through *Riftia* gill (Goffredi et al., 1997, 1999b). It is therefore interesting that in the branchial epidermis, CA messenger RNA as well as CA protein are mainly localized in the pinnules and in the apical part of the epidermis, in close contact with surrounding seawater.

V-$H^+$ATPase generates both electrochemical and pH gradient across the endo- and exomembranes of eukaryote cells (Nelson, 1992), and is thus involved not only in acidifying endosomes but also the cell environment. In *Riftia* plume, the epidermal cells appeared to possess a V-$H^+$ATPase only at their apical membrane and in intracellular vesicles located mainly in the apical part of the cell cytosol. This repartition could induce local decreases of pH mediated by massive proton excretion, and shift the boundary layer equilibrium such that $P_{CO_2}$ would increase, driving $CO_2$ across the membrane by diffusion. Such a proton elimination process could be greatly facilitated by the high concentrations of CA found in the pinnules. Indeed, CA efficiently contributes to internal pH regulation and regulation of the net entering $CO_2$ gradient in the circulating fluids by reversible interconversion of $CO_2$ into bicarbonate and protons (Goffredi et al., 1997). Thus, the dual role of cytoplasmic CA and V-$H^+$-ATPase, essential to sustain $CO_2$ influx while regulating intracellular pH, is fully compatible with the localization of both proteins revealed in this study.

### *$CO_2$ transport in the trophosome lobule*

Physiological studies have suggested a role for carbonic anhydrase in the bacteriocytes: the final consumers of $CO_2$ are the bacteria that use only molecular $CO_2$ (Scott et al., 1999), but the main form of inorganic carbon in the blood is bicarbonate (Toulmond et al., 1994), hence the need for conversion. CA activity in trophosome extracts is high (109 μmol $CO_2$ $g^{-1}$ $min^{-1}$; Goffredi et al., 1999b) and recent studies on isolated bacteriocytes have shown that inhibition of CA by acetazolamide induces both extra- and intracellular pH variations (De Cian et al., 2002).

The *in situ* hybridization experiments on whole *Riftia* sections showed that CA mRNA is intensely transcribed throughout the trophosome lobules. Bacteriocytes and peritoneal cells were labeled for CA mRNA and CA protein, the intensity of the labeling appearing higher in peritoneal cells than in bacteriocytes. But the differences in organelle content between the two cell types revealed by ultrastructural observations (Gardiner and Jones, 1993) may account for the difference in staining. The cytoplasm of the bacteriocytes is filled with bacteria and does not contain as much endoplasmic reticulum (RER) as the peritoneal cells, so transcriptional activity may be higher in the latter. They constitute a cell layer directly surrounding the multiple peripheral afferent vessels that bring $CO_2$ and other solutes to the symbionts, but the inner part of the lobule is also filled with capillaries inbetween the bacteriocytes. Our results with CA labeling, however, do not allow us to distinguish any variation of the staining between the peripheral bacteriocytes and the central ones. Further investigations should be done using more sensitive techniques allowing quantitative analysis of the labeling, through the use of confocal microscopy and fluorescence quantification analysis software.

Immunohistological localizations of the ion pumps showed that, in trophosome sections, V-$H^+$ATPase was colocalized with CA immunolabeling at the cellular level in the bacteriocytes, but the peritoneal cells were free of staining. $Na^+K^+$-ATPase immunostaining was also limited to bacteriocytes.

The branchial epidermis and the bacteriocytes of *Riftia* appear to highly express vacuolar-type proton-pumping V-$H^+$ATPase both on intracellular vesicles and on specific domains of their plasma membrane. They also contain high levels of cytosolic carbonic anhydrase (CA). In addition to the $Na^+K^+$-ATPase localized herein, future investigation should focus on $HCO_3^-$ exchange processes present in *Riftia*. $HCO_3^-$ generated intracellularly in the branchial cells has to be actively transported across the plume epithelium to the circulating fluids, and then from the circulating fluids to the bacteriocyte cytosol. Attempts to identify a $Cl^-/HCO_3^-$ anion exchanger analog to Band-3 in the tissues of *Riftia* through histological and molecular biology approaches have failed (M.-C. De Cian and A. C. Andersen, unpublished results), which is not surprising since Band-3 is absent from red blood cells of lower vertebrates such as lamprey (Bogdanova et al., 1998; Hagerstrand et al., 1999; Cameron et al., 2000) and hagfish (Peters et al., 2000), and exhibits a different structure from mammals when present in kidney, liver and muscles of these species. However, evidence for different types of anion exhangers has been obtained in invertebrates, such as the $Na^+$-coupled $Cl^-/HCO_3^-$ exchanger, newly described in *Drosophila* (Romero et al., 2000). This transporter exchanges $Na^+$ and $HCO_3^-$ (or another anion) against $Cl^-$ and $H^+$ and requires a sustained gradient for $Na^+$, so may constitute an interesting alternative and should be investigated in *Riftia*.

### *Conclusion*

The present study has enhanced the importance of CA in two tissues of *Riftia pachyptila* involved in ion exchange, the branchial plume, particularly the symbiotic tissue, the trophosome, in carbon transport and conversion, pH regulation and ionic balance. Interestingly, as described in the cnidarian/algal association (Weis et al., 1989), the cytosolic CA localized in *Riftia* belongs to the α-CA gene family, according to the nucleotide sequence obtained, and not the bacterial γ-CA family. Reynolds et al. (2000) showed that the upregulation of CA gene is a function of symbiosis, since CA expression is enhanced in the presence of symbiotic algae in the host tissue. Since *Riftia* acquires symbionts at each generation after metamorphosis, it would be of interest to investigate the regulation of CA expression in *Riftia* as a function of larval development, and acquisition of the symbiosis by the worm through *in situ* hybridization and immunolocalization. The study of the establishment and regulation of the expression of the related ATPases in the plume and trophosome cells under a variety of physiological stimuli which modify proton transport and related ion-transport processes would also open new perspectives.

Funding for this project was provided by the French Research Department and a DORSALE grant. The authors wish sincerely to thank Julia Morales, Marie Knockaert and Sandrine Boulben for useful assistance and advice concerning immunoblot assays (CNRS-UPMC Roscoff, France). We also are grateful to Dr Paul Linser of the Whitney Laboratory at the University of Florida for generously providing the anti-CA II antibody used in this study, and the Developmental Studies Hybridoma Bank for providing the monoclonal antibodies. Finally, we acknowledge the contributions of the captains and crews of the *R. V. Atalante* and the *D. S. V. Nautile*, which were used in the collection of our samples.

## References

**Andersen, A. C., Jolivet, S., Claudinot, S. and Lallier, F. H.** (2002). Biometry of the branchial plume in the hydrothermal vent tubeworm *Riftia pachyptila* (Vestimentifera; Annelida). *Can. J. Zool.* **80**, 320-332.

**Bradford, M. M.** (1976). A rapid and sensitive method for the quantification of microgram quantities of proteins utilizing the principle of protein-dye binding. *Anal. Biochem.* **72**, 248-254.

**Bogdanova, A. Y., Sherstobitov, A. O. and Gusev, G. P.** (1998). Chloride transport in red blood cells of lamprey *Lampreta fluviatilis*: evidence for a novel anion-exchange system. *J. Exp. Biol.* **201**, 693-700.

**Brion, L. P., Cammer, W., Satlin, L. M., Suarez, C., Zavilowitz, B. J. and Schuster, V. L.** (1997). Expression of carbonic anhydrase IV in carbonic anhydrase II-deficient mice. *Am. J. Physiol. Renal Physiol.* **42**, F234-F245.

**Cameron, B. A., Gilmour, K., Forster, R., Ko, K. and Tufts, B. L.** (2000). Unique distribution of the anion exchange protein in the sea lamprey, *Petromyzon marinus*. *J. Comp. Physiol. B* **170**, 497-504.

**Cavanaugh, C. M., Gardiner, S. L., Jones, M. L., Jannasch, H. W. and Waterbury, J. B.** (1981). Prokaryotic cells in the hydrothermal vent tube-worm *Riftia pachyptila* Jones: possible chemoautotrophic symbionts. *Science* **213**, 340-342.

**Chen, R. F. and Kernohan, J. C.** (1967). Combination of bovine carbonic anhydrase with a fluorescent sulfonamide. *J. Biol. Chem.* **24**, 5813-5823.

**Childress, J. J., Lee, R. W., Sanders, N. K., Felbeck, H., Oros, D. R., Toulmond, A., Desbruyères, D., Kennicut II, M. C. and Brooks, J.** (1993). Inorganic carbon uptake in hydrothermal vent tubeworms facilitated by high environmental $P_{CO_2}$. *Nature* **362**, 147-149.

**De Cian, M. C., Andersen, A. C., Toullec, J. Y., Biegala, I., Caprais, J. C.,**

**Shillito, B. and Lallier, F. H.** (in press). Isolated bacteriocyte cell suspensions from the hydrothermal vent tubeworm *Riftia pachyptila*, a potent tool for cellular physiology in a chemoautotrophic symbiosis. *Mar. Biol.*

**Dermietzel, R., Leibstein, A., Siffert, W., Zamboglou, A. and Gros, G.** (1985). A fast screening method for histochemical localization of carbonic anhydrase. *J. Histochem. Cytochem.* **33**, 93-98.

**Felbeck, H.** (1981). Chemoautotrophic potential of the hydrothermal vent tubeworm, *Riftia pachyptila* Jones (Vestimentifera). *Science* **213**, 336-338.

**Fisher, C. R., Childress, J. J. and Sanders, N. K.** (1988). The role of vestimentiferan hemoglobin in providing an environment suitable for chemoautotrophic sulfide-oxidizing endosymbionts. *Symbiosis* **5**, 229-246.

**Gardiner, S. L. and Jones, M. L.** (1993). Vestimentifera. In *Microscopic Anatomy of Invertebrates: Onychophora, Chilopoda and lesser Protostomata.*, vol. 12 (ed. S. L. Gardiner), pp. 371-460. New York: Wiley-Liss.

**Goffredi, S. K. and Childress, J. J.** (2001). Activity and inhibitor sensitivity of ATPases in the hydrothermal vent tubeworm *Riftia pachyptila*: a comparative approach. *Mar. Biol.* **138**, 259-265.

**Goffredi, S. K., Childress, J. J., Desaulniers, N. T., Lee, R. W., Lallier, F. H. and Hammond, D.** (1997). Inorganic carbon acquisition by the hydrothermal vent tubeworm *Riftia pachyptila* depends upon high external $P_{CO_2}$ and upon proton-equivalent ion transport by the worm. *J. Exp. Biol.* **200**, 883-896.

**Goffredi, S. K., Childress, J. J., Lallier, F. H. and Desaulniers, N. T.** (1999a). The ionic composition of the hydrothermal vent tube worm *Riftia pachyptila*: Evidence for the elimination of $SO_4^{2-}$ and $H^+$ and for a $Cl^-/HCO_3^-$ shift. *Physiol. Biochem. Zool.* **72**, 296-306.

**Goffredi, S. K., Girguis, P. R., Childress, J. J. and Desaulniers, N. T.** (1999b). Physiological functioning of carbonic anhydrase in the hydrothermal vent tubeworm *Riftia pachyptila*. *Biol. Bull.* **196**, 257-264.

**Hagerstrand, H., Danieluk, M., BobrowskaHagerstrand, M., Holmstrom, T., KraljIglic, V., Lindqvist, C. and Nikinmaa, M.** (1999). The lamprey (*Lampetra fluviatilis*) erythrocyte; morphology, ultrastructure, major plasma membrane proteins and phospholipids, and cytoskeletal organization. *Mol. Membr. Biol.* **16**, 195-204.

**Henry, R. P.** (1996). Multiple roles of carbonic anhydrase in cellular transport and metabolism. *Annu. Rev. Physiol.* **58**, 523-538.

**Henry, R. P. and Cameron, J. N.** (1982). The distribution and partial characterization of carbonic anhydrase in selected aquatic and terrestrial decapod crustaceans. *J. Exp. Zool.* **221**, 309-321.

**Henry, R. P., Gilmour, K. M., Wood, C. M. and Perry, S. F.** (1997). Extracellular carbonic anhydrase activity and carbonic anhydrase inhibitors in the circulatory system of fish. *Physiol. Zool*. **70**, 650-659.

**Jones, M. L.** (1981). *Riftia pachyptila* Jones: observations on the Vestimentiferan worm from the Galapagos rift. *Science* **213**, 333-336.

**Jones, M. L.** (1988). The Vestimentifera, their biology, systematic and evolutionary patterns. *Oceanol. Acta* **8**, 69-82.

**Just, F. and Walz, B.** (1994). Localization of carbonic anhydrase in the salivary glands of the cockroach, *Periplaneta americana*. *Histochem.* **102**, 271-277.

**Kochevar, R. E., Govind, N. S. and Childress, J. J.** (1993). Identification and characterization of two carbonic anhydrases from the hydrothermal vent tubeworm *Riftia pachyptila* Jones. *Mol. Mar. Biol. Biotechnol.* **2**, 10-19.

**Laemmli, U. K.** (1970). Cleavage of structural proteins during assembly of the head of bacteriophage T4. *Nature* **227**, 680-685.

**Lebovitz, R. M., Takeyasu, K. and Fambrough, D. M.** (1989). Molecular characterization and expression of the (Na-K)-ATPase α-subunit in *Drosophila melanogaster*. *EMBO J.* **8**, 193-202.

**Lucas, J. M. and Knapp, L. W.** (1996). Biochemical characterization of purified carbonic anhydrase from the octocoral *Leptogorgia virgulata*. *Mar. Biol.* **126**, 471-477.

**Lutz, R. A., Shank, T. M., Fornari, D. J., Haymon, R. M., Lilley, M. D., Vondamm, K. L. and Desbruyeres, D.** (1994). Rapid growth at deep-sea vents. *Nature* **371**, 663-664.

**Maren, T. H.** (1967). Carbonic anhydrase: chemistry, physiology and inhibition. *Phyiol. Rev.* **47**, 595-781.

**Nelson, N.** (1992). The vacuolar $H^+$-ATPase – one of the most fundamental ion pumps in nature. *J. Exp. Biol.* **204**, 25-37.

**Peters, T., Forster, R. E. and Gros, G.** (2000). Hagfish (*Myxine glutinosa*) red cell membrane exhibits no bicarbonate permeability as detected by $^{18}O$ exchange. *J. Exp. Biol.* **203**, 1551-1560.

**Reynolds, W. S., Schwarz, J. A. and Weis, V. M.** (2000). Symbiosis-enhanced gene expression in cnidarian-algal associations: cloning and characterization of a cDNA, sym 32, encoding a possible cell adhesion protein. *Comp. Biochem. Physiol.* **126A**, 33-44.

**Romero, M. F., Henry, D., Nelson, S., Harte, P. J., Dillon, A. K. and Sciortino, C. M.** (2000). Cloning and characterization of a $Na^+$-driven anion exchanger (NDAE1) – A new bicarbonate transporter. *J. Biol. Chem.* **275**, 24552-24559.

**Scott, K. M., Bright, M., Macko, S. A. and Fisher, C. R.** (1999). Carbon dioxide use by chemoautotrophic endosymbionts of hydrothermal vent vestimentiferans: affinities for carbon dioxide, absence of carboxysomes, and delta C-13 values. *Mar. Biol.* **135**, 25-34.

**Shillito, B., Lubbering, B., Lechaire, J. P., Childress, J. J. and Gaill, F.** (1995). Chitin localization in the tube secretion system of a repressurized deep-sea tube worm. *J. Struct. Biol.* **114**, 67-75.

**Toulmond, A., Lallier, F. H., De Frescheville, J., Desbruyères, D., Childress, J. J., Lee, R. and Sanders, N. K.** (1994). Unusual carbon dioxide-combining properties of body fluids in the hydrothermal vent tubeworm *Riftia pachyptila*. *Deep-Sea Res.* **41**, 1447-1456.

**Tufts, B. L., Gervais, M. R., Moss, A. G. and Henry, R. P.** (1999). Carbonic anhydrase and red blood cell anion exchange in the neotenic aquatic salamander, *Necturus maculosus*. *Physiol. Biochem. Zool.* **72**, 317-327.

**Weis, V. M.** (1991). The induction of carbonic anhydrase in the symbiotic sea anemone *Aiptasia pulchella*. *Biol. Bull.* **180**, 496-504.

**Weis, V. M., Smith, G. J. and Muscatine, L.** (1989). A '$CO_2$ supply' mechanism in zooxanthellate cnidarians: role of carbonic anhydrase. *Mar. Biol.* **100**, 195-202.